Discrimination of Coherent Features in Turbulent Boundary Layers by the Entropy Method

T.C. Corke* and Y.G. Guezennec†
Illinois Institute of Technology, Chicago, Illinois

Entropy in information theory is defined as the expected or mean value of the measure of the amount of self-information contained in the ith point of a distribution series x_i, based on its probability of occurrence $p(x_i)$. If $p(x_i)$ is the probability of the ith state of the system in probability space, then the entropy $E(X) = -\Sigma_{i=1}^{N} p(x_i)\log(p(x_i))$ is a measure of the disorder in the system. Based on this concept, a method was devised that sought to minimize the entropy in a time series in order to construct the signature of the most coherent motions. The constrained minimization was performed using a Lagrange multiplier approach that resulted in the solution of a simultaneous set of nonlinear coupled equations to obtain the coherent time series. The application of the method to space-time data taken by a rake of sensors in the near-wall region of a turbulent boundary layer was presented. The results yielded coherent velocity motions made up of locally decelerated or accelerated fluid having a streamwise scale of approximately $100\nu/u_\tau$, which is in qualitative agreement with the results from other less objective discrimination methods.

Introduction

RECENTLY there has been a central interest in the presence of organized coherent structures in turbulent flows. However, it is often difficult to detect these organized motions since their velocity signatures are not known a priori and are masked by incoherent velocity fluctuations. Blackwelder and Kaplan,[1] Willmarth and Lu,[2] Wallace, Eckelmann, and Brodkey,[3] and Johansson and Alfredsson,[4] to name a few, have identified coherent structures in wall-bounded shear flows by seeking predescribed features in a one-dimensional velocity time series. Most frequently, a threshold was also required in order to discriminate the "events" from the background noncoherent velocity fluctuations.

Corke[5] demonstrated that any technique that relies on the detection of events through locally large statistical quantities may be accepting only part of the total distribution of these events. In particular, setting a local threshold includes only events of a particular class that are sufficiently energetic or otherwise pass some biased criterion. Other events of the same class may exist but are ignored because they do not fall within narrow sampling criteria. That is to say that results based on such an approach must be qualified in a manner appropriate to the selection parameters. To overcome this limitation, the more recent work by Corke[5] in a turbulent boundary layer utilized one- and two-dimensional matched filtering for pattern recognition. In the one-dimensional case, however, an a priori velocity signature describing the event was needed as a "template" for the matched filter response.

In a two-dimensional approach, Townsend[6] and Mumford[7] utilized specific "model" velocity patterns in an attempt to bring out coherent patterns in the time series from a rake of velocity sensors placed in different shear flows. However, with the exception of the detection of circularly symmetric structures, this approach is prebiased on the translational or rotational orientation of the template feature. This was the motivation behind the more general use of the low-pass filters for two-dimensional match filtering of hot-wire rake data and flow visualization images presented by Wlezien[8] and Corke.[9]

Lumley[10] pointed out that "one can find in statistical data irrelevant structures with high probability which are formed by chance juxtaposition of other, relevant structures and in a physical sense have no significance." In this object lesson he draws the moral that it is dangerous to search for a rare "bird" in a random field. In his 1965 paper, Lumley[11] proposed an orthogonal decomposition technique as a means to determine more objectively the large-scale structures in a turbulent flow. By this technique, coherent eddies are identified by eigenvalues and eigenfunctions of the space-time correlations taken in a three-dimensional matrix grid in the flowfield. The lowest-order eigenfunctions correspond to the largest structures in the turbulent flow. Payne and Lumley[12] performed an eigenfunction decomposition of the space-time correlations of streamwise velocity fluctuations in the wall region of a turbulent boundary layer to obtain a dominant eigenfunction structure consisting of counterrotating eddy pairs of elongated streamwise extent.

Although this approach looks appealing, the amount of data necessary to carry out this sort of decomposition is large. If higher-order eigenfunctions are present, as we might expect in a turbulent jet flow (Drubka[13]), the amount of data required increases by an order of magnitude. In addition, the result of the orthogonal decomposition provides a space-time average view of the flow. By such a method, dominant low-order eigenfunctions that are alternating, as in the case of the axisymmetric and helical modes in the developing shear layer of a circular jet, will yield a smeared picture of the physical processes.

Based on these limitations, a method was sought that would allow the demarcation of the instantaneous signatures of coherent structures in an objective fashion. Another requirement for such a method was that it should not be sensitive to changes in statistical properties of the data that may arise from changing Reynolds number or temporal or spatial development of the coherent structures. In other words, the method must be data-adaptive.

Presented as Paper 84-0534 at the AIAA 22nd Aerospace Sciences Meeting, Reno, NV, Jan. 9-12, 1984; received May 31, 1984; revision submitted May 10, 1985.

*Assistant Professor, Department of Mechanical Engineering. Member AIAA.

†Graduate Assistant, Department of Mechanical Engineering.

Entropy

In the 1920s, there began attempts to develop a quantitative theory of the measure of information and to apply this measure to communications systems. Early pioneering efforts defined the information rate of a communications system as the logarithms of the number of possible messages that could be sent, assuming that all messages are equally likely. Further, the concept was formulated that both desirable and undesirable signals (noise) could be defined in probabilistic terms as random processes. Drawing on these, Shannon and Weaver[14] published their famous paper, "A Mathematical Theory of Information," in which they introduced the concepts of entropy and channel capacity in communications systems.

In information theory, the concern is with the relative frequency of occurrence of messages and not with their meaning. If we presume that every member of a message set is expressible by means of some combination of a finite set of values, then we can denote a set $[X]$ with elements x_1, $x_2,...x_N$, where N is the total number of values that can be taken. In probability space $p(x_i)$, $i=1,2,...,N$ is the probability of occurrence of the ith symbol x_i. A measure of the amount of self-information[14] contained in the ith symbol x_i based on the probability $p(x_i)$, is

$$I(x_i)=\ell n[1/p(x_i)]$$

where $I(x_i)$ is a decreasing function of $p(x_i)$ with the endpoint values of infinity for the impossible event and zero for the certain event. The expected value, or mean, of the random variable $I(x_i)$ is

$$E(X)=-\sum_{i=1}^{N} p(x_i)\ell n[p(x_i)]$$

where $E(X)$ is called the entropy of the distribution $p(x_i)$. If $p(x_i)$ is interpreted as the probability of the ith state of the system in probability space, then this expression is identical to the entropy of statistical mechanics and thermodynamics. Namely, $E(X)$ is a measure of the disorder in the system.

Coherent features in a time series will be associated with a high entropy as a measure of their organized structure. One can then develop a class of methods by which the given time series can be decomposed into a coherent part and a noncoherent part, the first one obeying a maximum entropy principle. Various researchers in the fields of optics, astrophysics, and geophysics have developed such methods to restore diffracted and noisy images or to analyze the data signature associated with earthquakes. Frieden[15] introduced the notion of configurational or spatial entropy, obtained by replacing the probability $p(x_i)$ by the data itself (x_i) in an expression similar to the statistical entropy introduced earlier, namely,

$$E(X)=-\sum_{i=1}^{N} x_i\ell nx_i$$

For large data sets, this definition is asymptotically equivalent to the one based on $p(x_i)$. Importantly, the use of the configurational entropy allows a more mathematically tractable set of equations, which are otherwise hard to express in terms of probability distributions. This will become more apparent in the next section.

Several restoration algorithms have been developed that use this quantity as an indication of the disorder in the data set and strive to converge to a solution having the maximum entropy. Frieden[15] and Gull and Daniel[16] describe such an application to radio astronomy. An important feature of the method, however, is that in all cases the unconstrained maximization of the entropy always leads to a constant time series (similar to the dc component), which is in fact the most ordered configuration. Although this is consistent with the method, it yields no new information. Therefore, in order to apply the method, it is necessary to require further that the coherent component be "consistent" with the given data set. The choice of the constraints used to enforce such consistency is where the various methods proposed in the literature differ. The determination of the appropriate constraints for a given type of problem is undoubtedly the heart of the maximum entropy method.

Formulation of the Problem

Let $[x_i]$, $i=1,2,...,N$ be a given time series. As mentioned earlier, we postulate that there exists a decomposition of the time series into a coherent part $[c_i]$ and a noncoherent part $[n_i]$, where the former obeys a maximum entropy principle, i.e.,

$$x_i=c_i+n_i$$

The c_i's have been assumed all positive without loss of generality. (If this is not the case, a constant can be added to the time series to satisfy such a requirement.) The n_i's can be positive or negative.

We are seeking the c_i's such that the entropy associated with this time series is a maximum, i.e.,

$$E(C)=-\sum_{i=1}^{N} c_i\ell nc_i=\text{Maximum}$$

Constraints must be imposed on the maximization procedure to yield a result that is consistent with the given time series. The choice of constraints is governed by the a priori knowledge of the physics of the problem and should be global, such as statistical measures, rather than punctual, such as thresholds.

Given the statistical nature of the turbulent signals, it was felt that the consistency required between the original turbulent signal and its coherent component should be imposed through constraints on their respective probability distribution functions. After careful experimentation, constraints on the first three moments of the probability density functions were found sufficient to enforce that consistency, i.e., to keep the character of the signals similar in a global sense. Constraining moments higher than the third moment only resulted in a stiffer set of equations and otherwise did not appreciably affect the outcome of the entropy processing. By this choice of constraints, we expect the coherent part to have a significant amount of energy compared to the total, but this does not require that the noncoherent part have zero values for the first three moments. Importantly, we do not enforce a particular time scale or pattern by this choice of constraints. In addition, since the statistical moments are not a function of the order in which we process the data, it is an easy extension of the method to go from one-dimensional to multidimensional data sets.

The problem was then cast into a minimization problem by reversing the sign of the entropy and using a Lagrange multiplier approach to enforce the constraints. Hence, we seek to find the c_i's that minimize the following functional:

$$F=\sum_{i=1}^{N} c_i\ell nc_i+\mu\left[\sum_{i=1}^{N} c_i-\sum_{i=1}^{N} x_i\right]+\nu\left[\sum_{i=1}^{N}(c_i-\bar{c})^2-\sum_{i=1}^{N}(x_i-\bar{x})^2\right]+\lambda\left[\sum_{i=1}^{N}(c_i-\bar{c})^3-\sum_{i=1}^{N}(x_i-\bar{x})^3\right]$$

where λ, μ, and ν are Lagrange multipliers and $\bar{c}$ and $\bar{x}$ the mean values of the c_i's and x_i,'s respectively.

Differentiation of this functional with respect to the c_i's and the Lagrange multipliers leads to a set of $(N+3)$

nonlinear coupled equations with $(N+3)$ unknowns where, again, N is the number of sampled values in the time series. The resulting set of equations is as follows:

$$1+\ell nc_i+2\nu(c_i-\bar{c})+\mu+3\lambda(c_i-\bar{c})^2=0$$

$$\sum_{i=1}^{N} c_i-\sum_{i=1}^{N} x_i=0$$

$$\sum_{i=1}^{N}(c_i-\bar{c})^2-\sum_{i=1}^{N}(x_i-\bar{x})^2=0$$

$$\sum_{i=1}^{N}(c_i-\bar{c})^3-\sum_{i=1}^{N}(x_i-\bar{x})^3=0$$

Attempts were made to solve this system by a conventional Newton-Raphson algorithm. However, that method was found extremely sensitive to the initial guess in the iterative solution technique, and convergence was achieved only in very controlled cases. This lead to the choice of a quasi-Newton method developed by Broyden,[17] which exhibits a wider radius of convergence. The method also presents some computational advantages, such as not computing the Jacobian of the nonlinear operator at each iteration but rather utilizing a predictor/corrector updating. The method is very insensitive to the initial starting values but possesses quadratic convergence properties near the solution, hence remaining computationally efficient. This former characteristic of the Broyden method is important since in the most objective approach we have no a priori guess as to the solution. As a matter of practice, the unit matrix was used as an initial guess for the Hessian matrix and the given time series as an initial guess for the coherent time series.

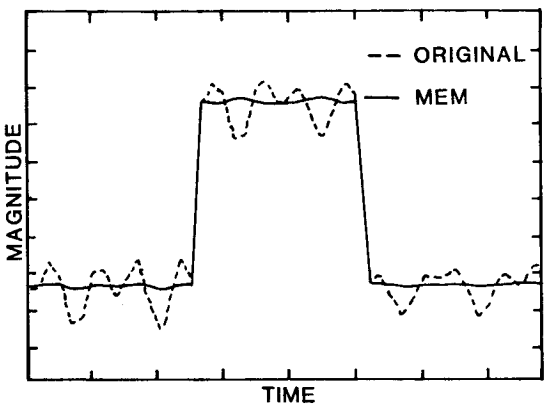

Fig. 1 Reconstruction of noise-degraded square wave by entropy processing.

Results

In order to develop an appreciation for the behavior of the method, we conducted a careful study utilizing synthetic time series data. Such test cases consisted of time series of known character such as square waves and sine waves, onto which was added random noise of various amplitudes. An example of one such test case is presented in Fig. 1. In this figure, the dashed line marks a data series made up of a square-wave pulse with 30%, by amplitude, additive random noise. The solid line marks the coherent component extracted by minimizing the positive entropy subject to the constraints listed earlier. Similar results were achieved in the other test cases examined.

The method was next applied to time-series data taken in turbulent boundary layers over a range of momentum thickness Reynolds numbers from 2000 to 5500. The data consisted of the streamwise component of velocity obtained in an Eulerian frame from a single hot-wire sensor or from a multiple sensor rake. The measurements were taken at different heights and streamwise stations along the boundary-layer plate, shown schematically in Fig. 2. These velocity time-series were digitally sampled and stored on digital magnetic tape for later processing.

Two different realizations of the velocity time series at $y^+=15$ taken at station 1 (see Fig. 2), at a Reynolds number of 2000, are shown in Fig. 3. The dashed traces correspond to the unprocessed 100-point data sets covering approximately 400 ν/u_τ^2 s. The solid traces correspond to the coherent part of the minimized entropy results. These two particular cases were chosen for presentation here because they exhibited quite different character even though they are from the same boundary-layer and measurement location. For example, the realization in the top part of the figure appears to have a decaying trend in it that is properly preserved in the minimum entropy result. The variability exhibited here between the unprocessed time traces demonstrates the need for such data adaptive methods. Simple thresholds or filter cutoffs may reject "important" events of the same class.

To demonstrate that the method is not a simple frequency filtering, we chose in Fig. 4 to compare a sample time series taken in the boundary layer under the same conditions as in Fig. 3, which was either processed using the minimum entropy or low-pass-filtered using either of two stop-band cutoff frequencies. Focusing on the large double-peaked feature near the center of the time trace, we note that a suitably selected low-pass cutoff frequency, in the middle figure, yields a trend similar to that obtained for the entropy-processed result at the top. The region of sharp deceleration on the left in the time series, however, is completely suppressed by the low-pass filter, whereas the entropy-processed result shows it to be somewhat amplified, owing to its significance to that data set. The constant value regions at the left and right of the filtered traces is a result of

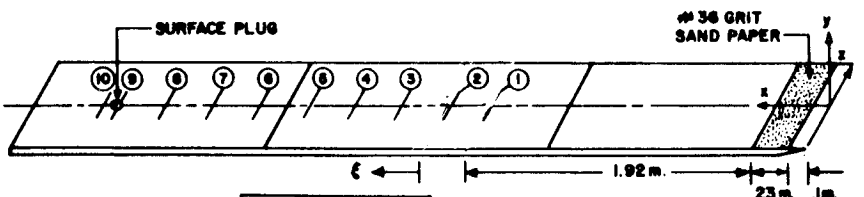

STATION#	X (m)
1	2.25
2	2.46
3	2.76
4	3.07
5	3.37
6	3.68
7	3.98
8	4.09
9	4.59
10	4.68

Fig. 2 Schematic of boundary-layer plate showing measurement stations and vertical rake of hot-wire sensors.

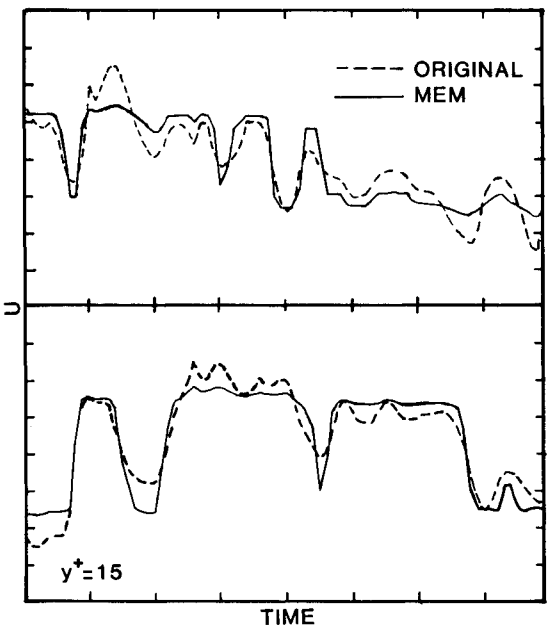

Fig. 3 Two realizations of velocity time series in near wall of turbulent boundary layer and coherent part (solid line) after entropy processing.

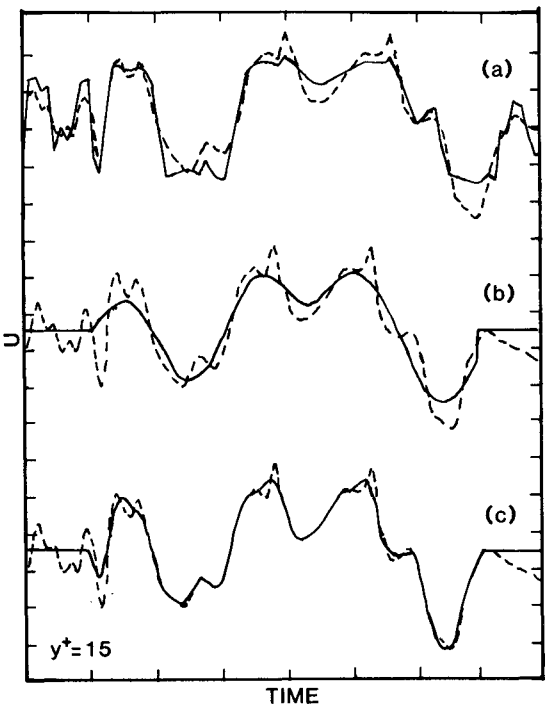

Fig. 4 Comparison of results of entropy processing (a) and low-pass filtering (b,c) with different stop-band cutoff frequencies.

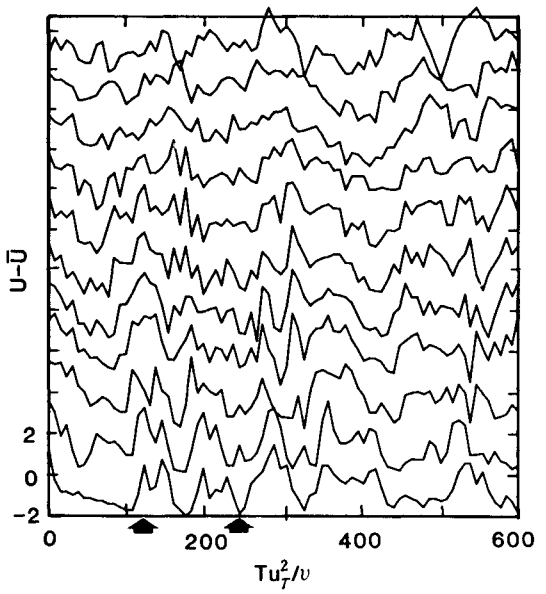

Fig. 5 Two realizations of space-time velocity series in near-wall region of turbulent boundary layer.

filter startup and is not relevant to the discussion. A suitable choice of a stop-band frequency cutoff necessary to retain the sharp deceleration in the left portion of the time trace results in little change from the original data set, as shown in the bottom part of the figure.

In order to better resolve the coherent three-dimensional motions in the near-wall region of the boundary layer, the space-time velocity data obtained using the rake of hot-wire sensors was examined. The data was acquired at station 9, where the Reynolds number was approximately 3300. The sensors spanned the boundary layer in the vertical direction over a range of y^+ values from 7 to 500. The results for this case are shown in Fig. 5. Although the sensors were spaced progressively closer in the region of higher mean shear near the wall, the mean-removed time traces were displayed in this figure to start from equally spaced origins. These normalized time traces correspond to one of a large number of statistically independent realizations that have been stored on digital magnetic tape as a record of the velocity fluctuations viewed in an Eulerian frame for approximately 600 ν/u_τ^2 s in the flow. We will focus on two regions in Fig. 5 that are centered about the arrows and that are continuous in time. These two regions are replotted as the two-dimensional arrays in Fig. 6. These arrays were formed by taking every fourth time-series point so as to form a 12- by 10-point set, each covering approximately 125 ν/u_τ^2 s in each trace. The sparsely sampled 12 by 10 array, requiring the solution of 123 simultaneous equations for 123 unknowns, was the largest set that could be efficiently processed in the PDP-11/34-based system available for the work. The results to follow, although limited in their temporal resolution, are meant to demonstrate the method and show the consistency with the processed one-dimensional time series presented in earlier figures.

The constrained minimization of the entropy of the space-time velocity variations in the arrays of Fig. 6 yields the respective results in Fig. 7. Examination of the results indicates a number of scales of motions, including a slender inclined feature formed by locally higher velocity fluid in the left portion of the figure. In order to better to view these results, the data in Fig. 7 are replotted as contours of constant normalized velocity in Fig. 8. The sparse data sets were interpolated using a two-dimensional spline function having a minimum amount of damping so as to not filter the results. In addition, the log was taken in the spatially sampled direction so as to space more evenly the sensor heights in the array. The y^+ value at the topmost sensor is approximately 500. In the figure, the dashed contours outline features moving at a streamwise speed less than the mean, and the solid contours outline features moving faster than the local mean velocity. Although processed separately, excellent continuity exists between features lying in the interface between the sample regions. This indicates that the probability statistics, on which the method is based, were reasonably ergodic for these few points.

When viewed in the manner of Fig. 8, the entropy-processed results show a repeating series of sharply decelerating and accelerating motions. The "burst" process

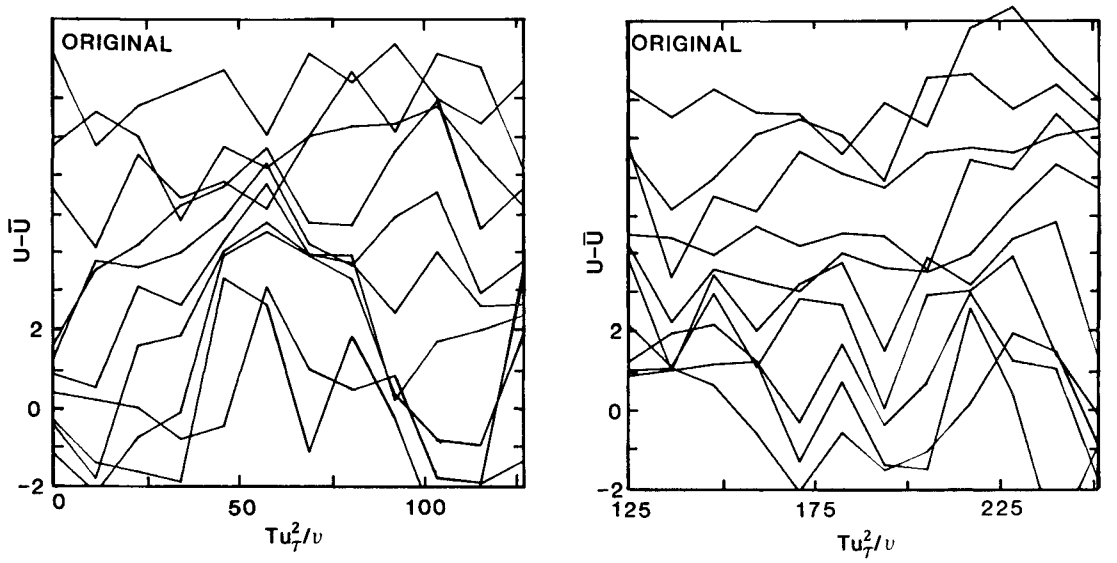

Fig. 6 Contiguous realizations of unprocessed space-time velocity series.

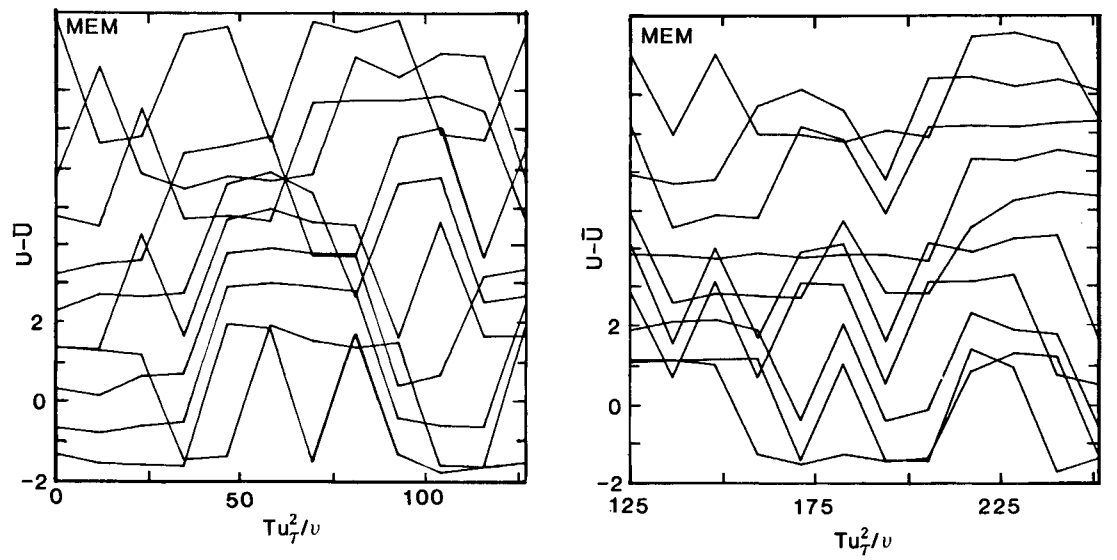

Fig. 7 Contiguous realizations of Fig. 6 after entropy processing.

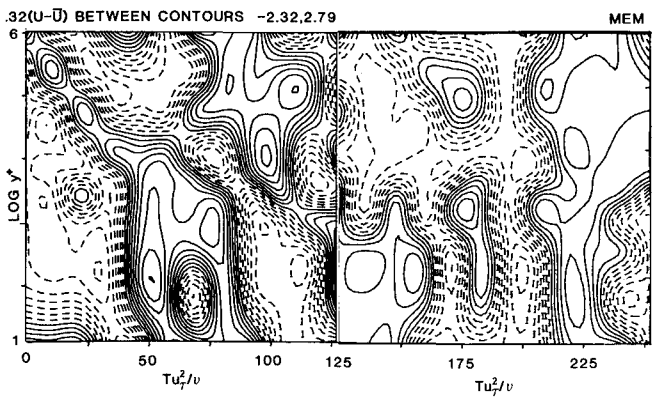

Fig. 8 Contours of constant normalized velocity of space-time arrays of Fig. 7.

defined by Blackwelder and Kaplan,[1] which consists of a one-dimensional velocity signature made up of a rapid deceleration/acceleration, would correspond to adjacent dashed/solid features in the representation in Fig. 8. However, the frequency of events, determined by the VITA technique,[1] would vary as a result of the threshold dependence of that method.

To better interpret the results of the entropy processing, the velocity histograms for the two arrays in Figs. 6 and 7 are presented in Fig. 9. Despite the relatively few samples, the unprocessed data, indicated by the dashed line, have a fairly broad distribution of velocity fluctuations. The coherent part of the processed data, however, exhibits a fairly bimodal distribution. This indicates that the coherent velocity fluctuations brought out by this method are made up primarily of shear layers bounded by relatively slow-moving fluid and relatively fast-moving fluid.

This view is consistent with the space-time velocity reconstructions obtained by Corke[5] and shown in Fig. 10. This consists of two-dimensionally low-pass-filtered velocity arrays of the type previously shown in Fig. 5 and presented as perturbation velocity contours in a manner consistent with the results in Fig. 8. The results from the entropy processing and the less objective, but more computationally efficient, spatial filtering indicate that the near-wall region of a turbulent boundary layer is in a bistable state of localized decelerating and accelerating fluid motions. This behavior is reminiscent of the model for the wall layer proposed many

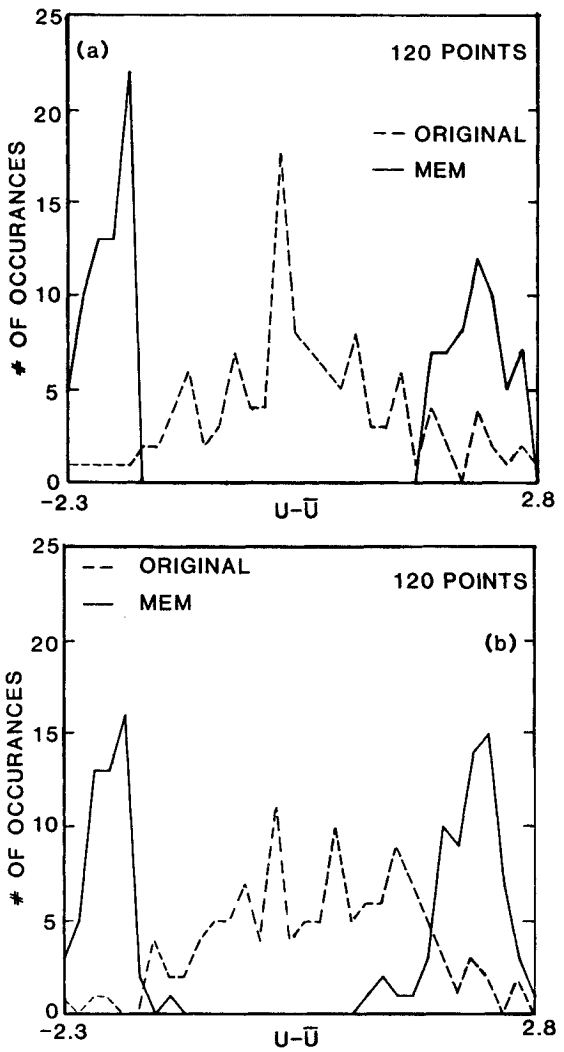

Fig. 9 Velocity histograms of entropy-processed and unprocessed space-time arrays.

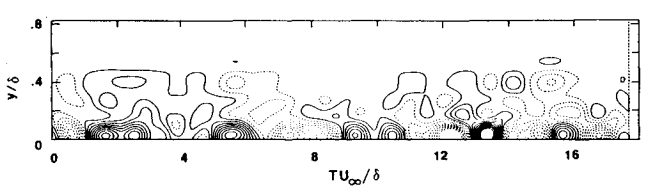

Fig. 10 Two-dimensional low-pass-filtered reconstructions of normalized streamwise velocity time series in near-wall region of turbulent boundary layer.

years earlier by Black,[18] Einstein and Li,[19] and Hanratty,[20] who considered the flow to be in a constant state of dissipation and regeneration. The frequency of these motions of the type exhibited in Fig. 10 have been correlated with the boundary-layer parameters by Corke.[5]

Concluding Remarks

The results presented here demonstrate the potential of the entropy method for extracting the coherent content from a data set in the objective manner. The key to this method has been the choice of constraints that are physically related to the fluid mechanics involved. The particular choice of constraints presented here has yielded results in the near-wall region of a turbulent boundary layer that are consistent with the physical picture brought out by other, less objective methods. The chief advantage of this method stems from the absence of any preconceived local patterns or criteria, making it a truly signal adaptive processing technique.

Acknowledgment

This work was sponsored under NASA Langley Research Center Grant NSG-1591.

References

[1]Blackwelder, R.F. and Kaplan, R.E., "On the Wall Structure of the Turbulent Boundary Layer," *Journal of Fluid Mechanics*, Vol. 76, Pt. 1, 1976, pp. 89-112.

[2]Willmarth, W.W. and Lu, S.S., "Structure of the Reynolds Stress Near the Wall," *Journal of Fluid Mechanics*, Vol. 55, Pt. 1, 1972, pp. 65-92.

[3]Wallace, J.M., Ecklemann, H., and Brodkey, R.S., "The Wall Region in Turbulent Shear Flow," *Journal of Fluid Mechanics*, Vol. 54, Pt. 1, 1972, pp. 39-48.

[4]Johansson, A. and Alfredsson, P., "On the Structure of Turbulent Channel Flow," *Journal of Fluid Mechanics*, Vol. 122, 1982, pp. 295-314.

[5]Corke, T.C., "A New View on the Origin, Role and Manipulation of Large Scales in Turbulent Boundary Layers," Ph.D. Thesis, Illinois Institute of Technology, Chicago, 1981; also NASA CR-165861.

[6]Townsend, A.A., "Flow Patterns of Large Eddies in a Wake and in a Boundary Layer," *Journal of Fluid Mechanics*, Vol. 95, Pt. 3, 1974, pp. 515-537.

[7]Mumford, J.C., "The Structure of Large Eddies in Fully Developed Turbulent Shear Flows," *Journal of Fluid Mechanics*, Vol. 118, 1982, pp. 241-268.

[8]Wlezien, R.W., "The Evolution of the Low Wave Number Structure in a Turbulent Wake," Ph.D. Thesis, Illinois Institute of Technology, Chicago, 1981.

[9]Corke, T.C., "Digital Image Filtering in Visualized Boundary Layers," *AIAA Journal*, Vol. 22, Aug. 1984, pp. 1124-1131.

[10]Lumley, J., "Coherent Structures in Turbulence," *Proceedings of Workshop on Stability and Transition*, Madison, WI, 1981.

[11]Lumley, J., "Atmospheric Turbulence and Radio Wave Propagation," *Proceedings of International Colloquium*, Moscow, 1965.

[12]Payne, F. and Lumley, J., "Large Eddy Structure of the Turbulent Wake Behind a Circular Cylinder," *Physics of Fluids Supplement*, 1967, pp. S194-S196.

[13]Drubka, R.E., "Instabilities in Near Field of Turbulent Jets and Their Dependence on Initial Conditions and Reynolds Number," Ph.D. Thesis, Illinois Institute of Technology, Chicago, 1981.

[14]Shannon, B. and Weaver, W., *A Mathematical Theory of Information*, University of Illinois Press, Urbana, 1949.

[15]Frieden, B., "Restoring with Maximum Likelihood and Maximum Entropy," *Journal of the Optical Society of America*, Vol. 62, No. 4, 1972, pp. 511-518.

[16]Gull, S.F. and Daniell, G.J., "Image Reconstruction from Incomplete and Noisy Data," *Nature*, Vol. 272, No. 20, 1978, pp. 686-690.

[17]Broyden, C.G., "A Class of Methods for Solving Nonlinear Simultaneous Equations," *Mathematical Computation*, Vol. 19, No. 92, 1965, pp. 577-593.

[18]Black, T.J., "The Structure of the Wall Turbulence," *Proceedings of Heat Transfer and Fluid Mechanics*, 1966, p. 366.

[19]Einstein, H.A. and Li, H., "The Viscous Sublayer Along a Smooth Wall," *ASCE Proceedings*, 82, 1956.

[20]Hanratty, T.J., "Turbulent Exchange of Mass and Momentum with a Boundary," *Journal of the American Institute of Chemical Engineering*, Vol. 2, 1956, p. 359.